Cellular Signalling xxx (2013) xxx–xxx

Contents lists available at ScienceDirect

Cellular Signalling

journal homepage: www.elsevier.com/locate/cellsig

Structural basis for the design of selective phosphodiesterase 4B inhibitors☆

David Fox III [a], Alex B. Burgin [a], Mark E. Gurney [b,c]

[a] Emerald Bio, Bainbridge Island, WA, USA
[b] Tetra Discovery Partners, Grand Rapids, MI, USA
[c] Basic Pharmaceutical Sciences, West Virginia University, Morgantown, WV, USA

ARTICLE INFO

Article history:
Received 4 November 2013
Received in revised form 4 December 2013
Accepted 11 December 2013
Available online xxxx

Keywords:
Phosphodiesterase-4B
PDE4B
Inhibitor
Control helix
Anti-inflammatory

ABSTRACT

Phosphodiesterase-4B (PDE4B) regulates the pro-inflammatory Toll Receptor –Tumor Necrosis Factor α (TNFα) pathway in monocytes, macrophages and microglial cells. As such, it is an important, although under-exploited molecular target for anti-inflammatory drugs. This is due in part to the difficulty of developing selective PDE4B inhibitors as the amino acid sequence of the PDE4 active site is identical in all PDE4 subtypes (PDE4A-D). We show that highly selective PDE4B inhibitors can be designed by exploiting sequence differences outside the active site. Specifically, PDE4B selectivity can be achieved by capture of a C-terminal regulatory helix, now termed CR3 (Control Region 3), across the active site in a conformation that closes access by cAMP. PDE4B selectivity is driven by a single amino acid polymorphism in CR3 (Leu674 in PDE4B1 versus Gln594 in PDE4D). The reciprocal mutations in PDE4B and PDE4D cause a 70–80 fold shift in selectivity. Our structural studies show that CR3 is flexible and can adopt multiple orientations and multiple registries in the closed conformation. The new co-crystal structure with bound ligand provides a guide map for the design of PDE4B selective anti-inflammatory drugs.

1. Introduction

Studies of targeted PDE4 gene deletions in mice by Jin and Conti, as well as others, have shown that the different PDE4 enzymes have non-redundant functions [1–6]. PDE4 is encoded by four different genes (PDE4A, PDE4B, PDE4C and PDE4D). These differ in their pattern of expression in the body, and differ in their pattern of targeting to subcellular compartments. The PDE4 family are the primary cAMP hydrolyzing enzymes in cells, and as such, shape the spatial and temporal patterning of cAMP signaling within cellular microdomains.

PDE4B is a well-validated target for modulating inflammation. For example, tumor necrosis factor (TNF-α) production by macrophages in response to an inflammatory stimulus is mediated by the Toll receptor pathway through an increase in PDE4B gene expression [2,3]. The increase in PDE4B drives down cAMP levels in the macrophage, thereby causing an increase in TNFα production. PDE4B is the major PDE4 in macrophages, and deletion of PDE4B in mice blunts the production of TNFα in response to inflammatory stimuli. PDE4B selective inhibitors similarly suppress TNF-α production in rodent models [7]. PDE4B dysregulation may also be important in psychiatric disease [8].

Each PDE4 gene encodes multiple transcripts that produce three isoforms of the enzyme termed long, short and super short. Long isoforms of PDE4 contain two upstream control regions known as UCR1 and UCR2 (upstream conserved region 1 and 2). These form a negative regulatory module which is relieved by protein kinase A (PKA) phosphorylation of UCR1 in response to cAMP (Fig. 1A) [9]. Burgin et al. demonstrated that this negative regulation resulted from a control helix within the UCR2 domain that can close over the active site [10]. The "closed" UCR2 conformation was visualized by X-ray crystallography using small molecules that bound in the active site and simultaneously interacted with specific residues in UCR2, most importantly Phe196. This residue is not conserved among PDE4 genes. Instead, it is replaced by a tyrosine in PDE4A-C. This has allowed the discovery of a number of PDE4D selective inhibitors which exploit the UCR2 binding pose (*e.g.* RS25344, PMNPQ, and D159153).

In the absence of UCR2, we showed previously that PMNPQ captures a second, downstream C-terminal helix, now termed CR3 (Conserved Region 3). CR3 is present in the protein constructs used to crystallize the catalytic domain of PDE4 but is typically disordered within the crystal lattice presumably because the helix only weakly interacts with the catalytic domain by itself. CR3 is visible in a number of PDE4 catalytic domain structures (1F0J, 3HMV, 3W5E and 3KKT); however, the length of CR3 that is visible is variable as is the orientation of CR3 in the structure [11–13].

To better understand the role of CR3 in regulating PDE4 activity, we surveyed additional compounds that could bind and stabilize CR3 over the active site. We report here the analysis and X-ray crystal structure

Abbreviation: CR3, Control Region 3.

0898-6568/$ – see front matter © 2013 The Authors. Published by Elsevier Inc. All rights reserved.
http://dx.doi.org/10.1016/j.cellsig.2013.12.003

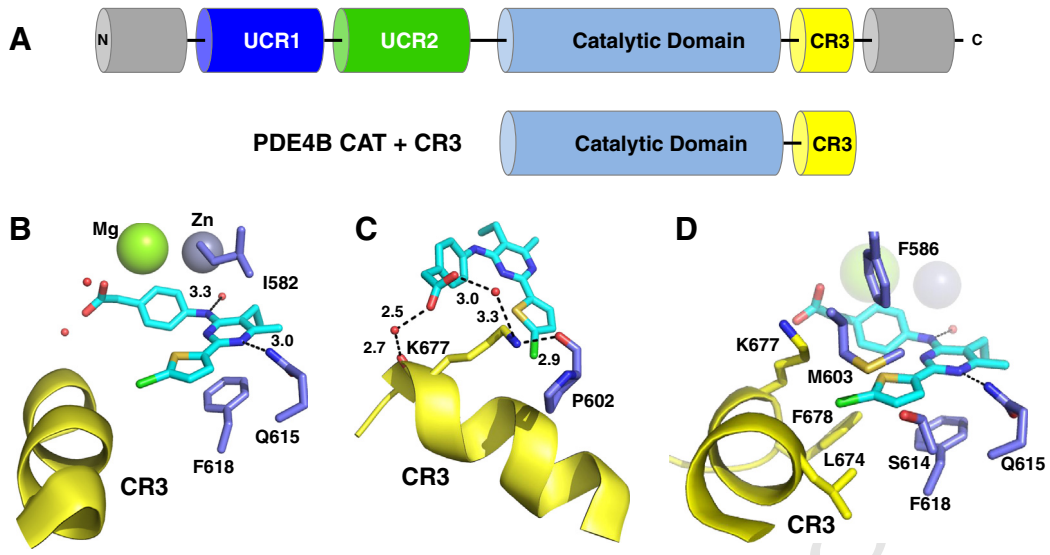

Fig. 1. PDE4B selective inhibitor captures the C-terminal CR3 by novel binding mode. A. Domain architecture for full-length PDE4 and the crystallization construct (PDE4B CAT + CR3). **B–D.** A-33 (cyan) interaction with catalytic domain (blue) and CR3 (yellow). **B.** "P-clamp" and "Q-switch." **C.** Hydrogen bonding network bridging CR3 and A-33 carboxylic acid. **D.** Hydrophobic interactions with A-33 thiophene. Atom coloring — Oxygen (red), Nitrogen (blue), Carbon (cyan), Chloride (green), and Sulfur (yellow). Metals are shown as large spheres (Mg^{2+} - green and Zn^{2+} - silver) and waters are shown as small red spheres. Hydrogen-bonds are represented by black dashed lines. PDB: 4MYQ.

of a previously described 2-arylpyrimidine [7] derivative (compound 33, herein referred to a A-33) bound to PDE4B. Comparison of this structure with the PMNPQ-PDE4D (PDB: 3G58), NVW-PDE4B (PDB: 3W5E), and OCP-PDE4B (PDB: 3KKT) structures, shows that small molecules can interact with different residues along the CR3 helix resulting in multiple "closed" conformations. The CR3 helix can adopt slightly different orientations across the active site, each with unique helical registries; however, only in the conformation observed in the new A-33 structure do the sequence differences between the PDE4B and PDE4D enzymes become critical for this interaction. In support of this model, we show that the reciprocal exchange of a single amino acid residue in CR3 between the PDE4B and 4D long isoforms can convert the selectivity profile of A-33 for PDE4B into that of PDE4D, and vice versa. These results demonstrate that CR3 can regulate PDE4 activity in biologically relevant PDE4 isoforms, and enable the first structure based drug design program of PDE4B selective inhibitors.

2. Materials and methods

2.1. PDE4 protein constructs

PDE4D residue numbering is based on the reference PDE4D3 isoform, GenBank accession No. AAA97892, and PDE4B residue numbering is on the reference PDE4B3, GenBank accession No. Q07343. Methods used to generate synthetic genes for human PDE4B1 (Swiss-Prot: Q07343.1) and PDE4D7 (GenBank: AAN10118.1) constructs are as described in Burgin et al. [10]. Mutations in the PDE4B1 (L674Q) and PDE4D7 (Q594L) constructs were cloned by site-directed mutagenesis of the respective long-form construct. A synthetic gene encoding the PDE4B catalytic domain and CR3 element (PDE4B-CR3, residues 324–691) with amino-terminal thrombin cleavable hexahistidine tag was engineered for Baculovirus-infected insect cell expression using Gene Composer™ software (Emerald Bio, Bainbridge Island, WA) [14]. The 389 amino acid fragment was cloned into a BV transfer vector, expression from which is driven by the polh promoter, using 5′ BamHI and 3′ HindIII.

2.2. Expression and purification of PDE4 proteins

PDE4 constructs were transfected into Sf9 insect cells (Expression Systems) using BestBac 2.0, v-cath/chiA Deleted Linearized Baculovirus DNA (Expression Systems). Virus from each transfection was amplified through 4 rounds to produce virus stock for large scale production. The large scale preparations were grown in ESF921 medium (Expression Systems) of approximately $2.5e^6$ cells per ml that was infected with 10% final virus (75 ml) and harvested 48 h post-infection. Cells were centrifuged to collect cell paste which was frozen drop-wise into liquid nitrogen and stored at −80 °C.

Frozen cell paste of the PDE4 long form and catalytic domain proteins was resuspended and lysed hypotonically in 20 mM tris(hydroxymethyl) aminomethane (Tris) pH 8.0 containing one complete protease inhibitor tablet for one hour at 4 °C. The lysate was clarified by centrifugation at 42 K rpm for 45 min at 4 °C. Sodium chloride (NaCl) was added to the clarified lysate to obtain a final concentration of 0.5 M. Clarified lysate was first purified by immobilized metal affinity chromatography with a HiTrap™ Chelating HP column and an AKTA FPLC system. The protein was eluted over a gradient with 20 mM Tris pH 8.0, 0.5 M NaCl and 0.5 M imidazole and the eluted fractions were analyzed via SDS-PAGE prior to pooling. Long-form PDE4 proteins were dialyzed into the final buffer containing 20 mM TRIS at pH 8.0, 0.1 M NaCl, 0.1 mM $MgCl_2$, 0.1 mM $ZnCl_2$, and 2 mM dithiothreitol (DTT) and then flash frozen with liquid nitrogen in aliquots of 0.5 mL at 0.1 mg/ml as measured by A_{280}. The PDE4B-CR3 protein eluted pool was further treated with thrombin to cleave the 6X His tag followed by removal of thrombin and the cleaved fusion tag by passing the cleaved pool over a benzamidine column and a HiTrap™ Chelating HP column in series. Cleaved PDE4B-CR3 was collected in the flow-through and dialyzed into the final buffer containing 20 mM 4-(2-hydroxyethyl)-1-piperazineethanesulfonic acid (HEPES) pH 7.5, 100 mM NaCl and 1 mM DTT. Cleaved PDE4B-CR3 was concentrated via centrifugal concentration to a final concentration of 7.9 mg/ml as measured by A_{280}. All proteins were stored at −80 °C.

2.3. Co-crystallization of PDE4B with A-33

Crystals of PDE4B-CR3 were grown by sitting drop vapor diffusion at 295 K using 0.5 μl of 7.9 mg/ml protein in the presence of 0.5 mM A-33 (DMSO) and combined with 0.5 μl of crystallization buffer containing 328.6 mM potassium formate, 24% w/v PEG 3,350 (based on JCSG$^+$ condition A10) [15]. Crystals grown for data collection were streak seeded using crystals described above and were cryo-protected using 20% ethylene glycol mixed with 0.1 mM A-33.

Please cite this article as: D. Fox, et al., Cellular Signalling (2013), http://dx.doi.org/10.1016/j.cellsig.2013.12.003